Journal of Solid State Chemistry 184 (2011) 888–892

Contents lists available at ScienceDirect

Journal of Solid State Chemistry

journal homepage: www.elsevier.com/locate/jssc

Phase diagram of $SrO–InO_{1.5}–CoO_x$ and a new compound $Sr_3In_{0.9}Co_{1.1}O_6$

Kuo Li [a], Denis Sheptyakov [b], Yingxia Wang [a,*], Chun-Keung Loong [a], Jianhua Lin [a,*]

[a] Beijing National Laboratory for Molecular Sciences, State Key Laboratory of Rare Earth Materials Chemistry and Applications, College of Chemistry and Molecular Engineering, Peking University, Beijing 100871, P R China

[b] Laboratory for Neutron Scattering, Paul Scherrer Institut, CH-5232 Villigen PSI, Switzerland

ARTICLE INFO

Article history:
Received 16 November 2010
Received in revised form
16 February 2011
Accepted 22 February 2011
Available online 26 February 2011

Keywords:
Complex oxides
Hexagonal perovskite
Neutron diffraction
Rietveld analysis
High spin Co^{3+}
Magnetic property

ABSTRACT

$Sr_3In_{0.9}Co_{1.1}O_6$, isostructural to $Ca_3Co_2O_6$, is revealed by the study of the phase relations in the system $SrO–InO_{1.5}–CoO_x$ (1000 °C). The structure of $Sr_3In_{0.9}Co_{1.1}O_6$ is refined by the combination of powder X-ray and neutron diffraction. $Sr_3In_{0.9}Co_{1.1}O_6$ crystallizes in a trigonal lattice with the cell parameters $a=b=9.59438(3)$ Å, $c=11.02172(4)$ Å with the space group $R\text{-}3c$. Its structure possesses 1D $(In/Co)O_3$ chains running along the c-axis constructed by alternating face-sharing CoO_6 octahedra and $(In_{0.9}Co_{0.1})O_6$ trigonal prisms. The co-occupation of In^{3+} and Co^{3+} at the trigonal prismatic site is evidenced by elementary analysis and determined by the structure refinement. $Sr_3In_{0.9}Co_{1.1}O_6$ is paramagnetic, and the susceptibility is consistent with the occupation of Co^{3+} at 10% of the trigonal prismatic positions in a high spin state (HS, $S=2$). The HS Co^{3+} is well separated by diamagnetic CoO_6 octahedra and InO_6 trigonal prisms and shows a g factor of 2.0 in the magnetic measurements.

1. Introduction

Hexagonal perovskite related compounds with the general formula $A_3B'BO_6$ have attracted considerable attention due to their interesting structural features and physical properties [1–8]. In this family, A is typically Ca or Sr, and B' and B can be the same, as in $Ca_3Co_2O_6$, or different cations, with B'=Y, Sc, In, Na, Mg, Ni, Cd, Zn, Co, Sm, Eu, Tb, Dy, Ho, Er, Tm, Yb, Lu, Pb, and B=Ru, Rh, Ir, Pd, Pt, Cr, Ni, Bi [6]. The structure of $A_3B'BO_6$ consists of infinite chains formed by alternating face-sharing $B'O_6$ trigonal prisms and BO_6 octahedra and each chain is surrounded by six chains separated by the A cations. These compounds possess quasi-1D structures in which the interaction within the chains is much stronger than that between the chains. Among them, $Ca_3Co_2O_6$ is a well investigated one [1,3,9–14]. It presents a ferromagnetic ordering of the magnetic Co^{3+} cations along the chains and antiferromagnetic correlations between chains at low temperature. Its magnetization curve displays steps at low temperature, which is considered as the result of interchain frustration. Due to the similar chemistry of Ca^{2+} and Sr^{2+} the larger size of Sr^{2+} accommodates more B and/or B' cations, so substitution of Ca^{2+} by Sr^{2+} results in a series of $Sr_3B'BO_6$ compounds [6].

In an effort to explore new compounds in the $Sr_3B'BO_6$ family, we focused on the system $SrO–InO_{1.5}–CoO$. In the related systems, no binary compound was revealed in the system $InO_{1.5}–CoO$, and only one compound, $SrIn_2O_4$, with a $CaFe_2O_4$-type structure was reported in $SrO–InO_{1.5}$ [15], while the system $SrO–CoO_x$ was complicated [5,7,16–22], in which $SrCoO_{2.52}$, $Sr_6Co_5O_{15}$, $Sr_5Co_4O_{12}$, $Sr_{24}Co_{19}O_{57}$, $Sr_4Co_3O_9$, $Sr_{14}Co_{11}O_{33}$, and $Sr_3Co_2O_{7-y}$ ($0.94 \le y \le 1.22$ were revealed. $SrCoO_{2.52}$ (JCPDF 40-1018) has an oxygen deficient hexagonal perovskite structure. $Sr_6Co_5O_{15}$, $Sr_5Co_4O_{12}$, $Sr_{24}Co_{19}O_{57}$, $Sr_4Co_3O_9$, and $Sr_{14}Co_{11}O_{33}$ belong to the hexagonal perovskite family Sr_xCoO_3 [6–7,18–22] and $Sr_3Co_2O_{7-y}$ ($0.94 \le y \le 1.22$) is an oxygen-deficient $n=2$ member of the Ruddlesden–Popper phase [23]. These strontium–cobalt complex oxides present various coordination configurations of cobalt, including octahedra, trigonal prisms, and intermediate polyhedra formed from octahedra and trigonal prisms, and accordingly there are a variety of magnetic and other physical properties [5,7,16–23].

This work presents the phase diagram of $SrO–InO_{1.5}–CoO_x$ at 1000 °C. A new ternary compound $Sr_3In_{0.9}Co_{1.1}O_6$, isostructural to $Ca_3Co_2O_6$, is revealed. In the 1D $B'BO_6$ chain formed by face-sharing octahedra and trigonal prisms, octahedral positions are fully occupied by Co^{3+} in the low spin state (LS, $S=0$) and trigonal prismatic positions are occupied by In^{3+} and Co^{3+} in the ratio of 9:1, where Co^{3+} are in the high spin state (HS, $S=2$) and well separated by In^{3+} and Co^{3+} (LS). This compound is paramagnetic due to the 10% occupancy of Co^{3+} (HS) in the trigonal prismatic positions.

2. Experimental

2.1. Materials and preparation

The samples were synthesized by conventional solid state reaction. $SrCO_3$, In_2O_3, and Co_3O_4 of analytical grade were mixed

* Corresponding authors: Fax: +86 10 62751708.
E-mail addresses: wangyx@pku.edu.cn (Y. Wang), jhlin@pku.edu.cn (J. Lin).

0022-4596/$ - see front matter © 2011 Elsevier Inc. All rights reserved.
doi:10.1016/j.jssc.2011.02.024

stoichiometrically and ground in an agate mortar. The mixture was calcined at 1000 °C under atmosphere for 3–5 days with several intermediate grindings and XRD examination. The samples in and near the SrO–CoO binary line were quenched in air. At the composition n_{Sr}:n_{In}:n_{Co}=3:1:1, a new compound was detected and it was revealed later that the product contained a small amount of $SrIn_2O_4$ impurity. The chemical and structural analysis indicates the new compound has a composition of $Sr_3In_{0.9}Co_{1.1}O_6$ and the experiment at the composition n_{Sr}:n_{In}:n_{Co}=3:0.9:1.1 gave rise to an almost pure phase.

2.2. Measurement and characterization

The powder XRD data for phase identification was collected in a Rigaku D/Max 2000 diffractometer using CuK_α radiation (λ=1.5418 Å) at room temperature(25 °C). The elementary analysis was carried out on an Inductively Coupled Plasma-Atomic Emission Spectrometer (ICP-AES). The sample obtained at the composition n_{Sr}:n_{In}:n_{Co}=3:1:1 was dissolved in 0.1 M HCl with a small amount of insoluble impurity $SrIn_2O_4$ remaining. After filtration, the solution was used for the ICP-AES analysis. Work curves were established in the analysis to calibrate the contents of In and Co. The molar ratio of In/Co in the solution corresponded to that in $Sr_3In_{0.9}Co_{1.1}O_6$. The oxidation state of cobalt in $Sr_3In_{0.9}Co_{1.1}O_6$, +2.98(2), was determined by iodimetric titration.

The powder XRD data used for structure determination was collected on a Bruker AXS D8 Discover X-Ray Diffractometer with CuK_α radiation (λ=1.5418 Å) and a graphite monochromator at the secondary beam. The powder neutron diffraction data was collected on the high resolution powder diffractometer for thermal neutrons (HRPT) of Swiss Spallation Neutron Source SINQ at the Paul Scherrer Institut, Switzerland, with the wavelength 1.494 Å at different temperatures (1.5, 4, 30, 60, 90, 120, 150,180, 210, 240, 270, 298 K). The electron diffraction patterns were taken on a JEOL JEM-2100 transmission electron microscope with an accelerating voltage of 200 kV and a camera length of 150 cm. The magnetic measurements were carried out on a Quantum Design MPMS-SS superconducting quantum interference device (SQUID) magnetometer in the temperature range 2–300 K at 0.1 T.

3. Results and discussion

3.1. Quasi-ternary phase diagram SrO–$InO_{1.5}$–CoO_x

The quasi-ternary phase diagram SrO–$InO_{1.5}$–CoO_x at 1000 °C under atmosphere is shown in Fig. 1. The cobalt oxide is CoO, under these conditions, and the oxidation state of cobalt varies in other cobalt-containing compounds. $SrIn_2O_4$ is observed in the SrO–$InO_{1.5}$ binary line. In the SrO–CoO_x system, $SrCoO_{2.52}$, $Sr_5Co_4O_{12}$, and $Sr_3Co_2O_{7-y}$ are identified, but $Sr_6Co_5O_{15}$, $Sr_4Co_3O_9$, $Sr_{14}Co_{11}O_{33}$, and $Sr_{24}Co_{19}O_{57}$ were not observed. $Sr_6Co_5O_{15}$ and $Sr_4Co_3O_9$ exist below ~900 and 940 °C, respectively [7,18–21], and $Sr_{14}Co_{11}O_{33}$ and $Sr_{24}Co_{19}O_{57}$ were previously obtained as single crystals grown from a mixture of $SrCO_3$, $CoCO_3$, and KOH in the Sr:Co:K molar ratio 1:1:10 [22]. $Sr_3Co_2O_{7-y}$ is not stable in air. It absorbs water quickly and then transforms to a hydrate phase [23]. With the substitution of Co by In, $Sr_3Co_2O_y$ extends to a solid solution $Sr_3Co_{2-x}In_xO_{7-\delta}$ ($0 \le x \le 0.27$) and $Sr_5Co_4O_{12}$ extends to $Sr_5Co_{4-x}In_xO_{7-\delta}$ ($0 \le x \le 0.56$).

There are four binary regions (A–D) and seven ternary regions (shown in different symbols) in the phase diagram, as depicted in Fig. 1. A new ternary compound, $Sr_3In_{0.9}Co_{1.1}O_6$, is identified. It exists as a sharp compound instead of a solid solution. The structure and properties of this compound are discussed in the following.

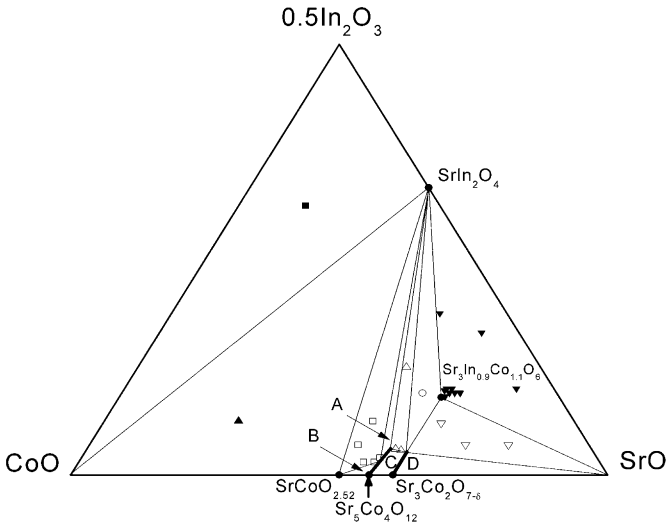

Fig. 1. Phase diagram of SrO–$InO_{1.5}$–CoO at 1000 °C in atmosphere. The two short black lines spreading from $Sr_5Co_4O_{12}$ and $Sr_3Co_2O_{7-\delta}$ indicate the In-substituted solid solution lines $Sr_5In_xCo_{4-x}O_{12}$ ($0 \le x \le 0.56$) and $Sr_3Co_{2-x}In_xO_{7-\delta}$ ($0 \le x \le 0.27$). Details of the binary phase region are shown in Fig. S1. The characters and symbols in the diagram are: (A) $SrIn_2O_4$+$Sr_5In_xCo_{4-x}O_{12}$ ($0.28 \le x \le 0.56$); (B) $SrCoO_{2.52}$ +$Sr_5In_xCo_{4-x}O_{12}$ ($0 \le x \le 0.28$); (C) $Sr_5In_xCo_{4-x}O_{12}$ ($0 \le x \le 0.56$)+$Sr_3Co_{2-x}In_xO_{7-\delta}$ ($0 \le x \le 0.27$); (D) $Sr_3Co_{2-x}In_xO_{7-\delta}$ ($0 \le x \le 0.27$)+SrO; (■) In_2O_3+CoO+$SrIn_2O_4$; (▲) $SrIn_2O_4$+CoO+$SrCoO_{2.52}$; (□) $SrIn_2O_4$+$SrCoO_{2.52}$+$Sr_5In_xCo_{4-x}O_{12}$ (x=0.28); (△) $Sr_5In_xCo_{4-x}O_{12}$ (x=0.56)+$Sr_3Co_{2-x}In_xO_{7-\delta}$ (x=0.27)+$SrIn_2O_4$; (▽) SrO+ $Sr_3Co_{2-x}In_xO_{7-\delta}$ (x=0.27)+$Sr_3In_{0.9}Co_{1.1}O_6$; (○) $Sr_3In_{0.9}Co_{1.1}O_6$+$SrIn_2O_4$+Sr_3Co_{2-x} $In_xO_{7-\delta}$ (x=0.27); (▼) $Sr_3In_{0.9}Co_{1.1}O_6$+$SrIn_2O_4$+SrO.

3.2. Structure of $Sr_3In_{0.9}Co_{1.1}O_6$

The indexing of the powder XRD data of $Sr_3In_{0.9}Co_{1.1}O_6$ by PowderX [24] shows a rhombohedral lattice with a=9.59 Å and c=11.02 Å in hexagonal expression, which is confirmed by electron diffraction patterns of a tilt series (Fig. 2). The peaks with $l=2n+1$ of $h-hl$ indices are all absent, indicating the existence of a c-glide; hence the space group R-3c is selected. Since the XRD pattern of $Sr_3In_{0.9}Co_{1.1}O_6$ is similar to that of $Ca_3Co_2O_6$, the atom coordinates of $Ca_3Co_2O_6$ were taken as the initial parameters for $Sr_3In_{0.9}Co_{1.1}O_6$ in the structure analysis. The structure parameters were refined by powder X-ray diffraction data and high resolution neutron diffraction data using the program Fullprof [25]. The Rietveld analysis results by X-ray are summarized in Tables S1 and S2 in the Supporting information. The data collection conditions and the results of Rietveld analysis by neutron data (298 K) are summarized in Table 1. The atomic coordinates, isotropic thermal factors, and occupancies (298 K) are listed in Table 2 and the selected bond lengths and angles are listed in Table 3. The Rietveld refinement plot of neutron data (298 K) is shown in Fig. 3. We also carried out the refinements using anisotropic thermal factors and the results from the neutron data (298 K) are provided in Table S3. The refined results of neutron data at 1.5 K are provided in Tables S4 and S5. The Rietveld refinement plots at 1.5 K, 30 K, and 180 K are provided in Figs. S2–Fig. S4 in the Supporting information. The variation of cell parameters of $Sr_3In_{0.9}Co_{1.1}O_6$ with temperature is listed in Table S6.

From the neutron diffraction data, the positions and the occupancies of oxygen atoms can be accurately determined. The structure refinement indicates that In^{3+} and Co^{3+} are located at the center of the trigonal prisms randomly in a ratio of 0.92(1):0.08(1) and all the octahedral positions are occupied by Co^{3+} atoms, which is consistent with the elementary analysis result n(In):n(Co)=0.91:1.09. It is noteworthy that we did not

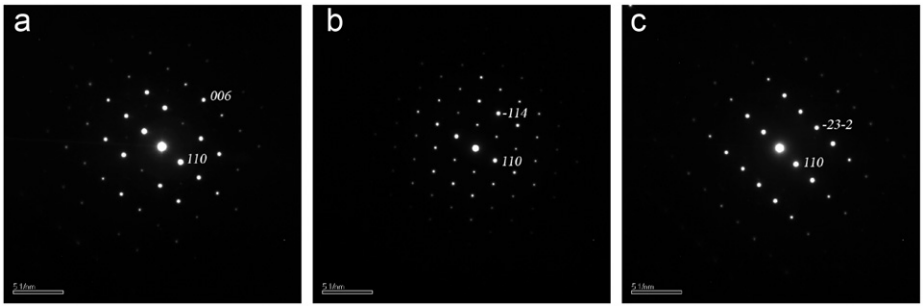

Fig. 2. Electron diffraction patterns of a tilt series of one crystallite for $Sr_3In_{0.9}Co_{1.1}O_6$ along the zone axes: (a) [1 −10]; (b) [2 −21]; (c) [−225].

Table 1
Neutron data collection conditions, crystallographic data and results of Rietveld analysis for $Sr_3In_{0.9}Co_{1.1}O_6$ (298 K).

Crystal data	
Chemical formula	$Sr_3In_{0.9}Co_{1.1}O_6$
M_r (g mol^{-1})	527.02
Space group (number)	*R*-3*c* (167)
Lattice parameters (Å, deg.)	a=9.59438(3), c=11.02172(4)
V (Å^3)	878.65(1)
Z	6
D_x (mg m^{-3})	5.97(1)
Radiation type, λ (Å)	Neutron (unpolarized), 1.494
μR	0.3
Data collection	
Diffractometer	High resolution powder diffractometer for thermal neutrons
Data collection method	Debye–Scherrer geometry
Specimen mounting	Vanadium container
Detector	PSD
Data collection mode	Transmission
2θ min., max., step (°)	5, 164.9, 0.05
Refinement	
R_p, R_{wp}, χ^2	0.030, 0.039, 4.25
$R_{expected}$	0.019
Excluded regions (°)	5.00–11.00
N−P+C	3047
Computer program	Fullprof 2009

Table 2
Atomic coordinates, occupancies and isotropic thermal displacement parameters for $Sr_3In_{0.9}Co_{1.1}O_6$ (298 K).

Atom	Wyckoff positions	*x*	*y*	*z*	Occupancy	$B_{eq.}$ (Å^2)
Sr	18*e*	0.3690(1)	0.00000	0.25000	1	0.49(1)
In	6*a*	0.00000	0.00000	0.25000	0.92(1)	0.49(4)
Co2	6*a*	0.00000	0.00000	0.25000	0.08(1)	0.49(4)
Co1	6*b*	0.00000	0.00000	0.00000	1	0.51(5)
O	36*f*	0.1713(1)	0.0211(1)	0.1100(1)	1	0.54(1)

observe any evidence of the simple stoichiometric compound "Sr_3InCoO_6", which reflects that the formation of the structure relies strongly on the radii of the $B(B')$-site cations.

The Co–O bond lengths and O–Co–O bond angles in the CoO_6 octahedra are consistent with the data previously reported for $Ca_3Co_2O_6$ [10]. Since the octahedron is elongated along the *c* direction, the Co^{3+} cation in this position has anisotropic thermal factors with $U33$=0.014 Å^2, $U11=U22$=0.003 Å^2 (See Table S3 and Fig. S5). The extrapolation of the thermal factors to 0 K shows that $U11$ and $U22$ tend to zero, but $U33$

Table 3
Selected bond distances (Å) and bond angles (deg.) for $Sr_3In_{0.9}Co_{1.1}O_6$ (298 K).

CoO_6 octahedra	
Co–O	1.970(1) × 6
O–Co–O	93.92(4) × 6;86.08(3) × 6
In(Co)O_6 trigonal prism	
In(Co)–O	2.189(1) × 6
O–In(Co)–O	90.37(4) × 3;75.80(3) × 6 130.12(4) × 3;147.10(5) × 3

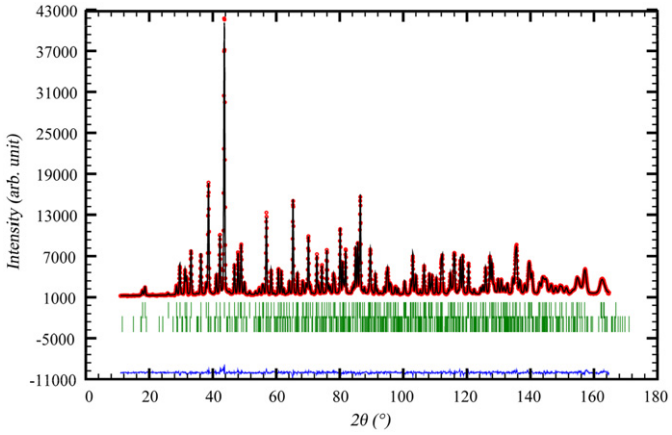

Fig. 3. Rietveld refinement plot of the powder neutron diffraction profile of $Sr_3In_{0.9}Co_{1.1}O_6$ at 298 K. The circles are the observed data and the solid line is for the calculated pattern, the marks below the diffraction pattern are reflection positions of $Sr_3In_{0.9}Co_{1.1}O_6$ (upper) and $SrIn_2O_4$ (lower, ~3 wt%), and the difference curve is shown at the bottom.

has a residual value of ~0.01 Å^2, which is generally considered to show the existence of a static displacive disorder in the structure [26]. In this case, it relates to the elongated extension of the CoO_6 octahedron along the *c* direction. For the InO_6 trigonal prism, the bond lengths and angles are reasonable. However, considering the occupation of Co^{3+} in trigonal prismatic positions, the space is quite large for a Co^{3+} cation, enabling the Co^{3+} to take the S=2 high spin state.

In the $Sr_3In_{0.9}Co_{1.1}O_6$ structure (Fig. 4), the chains are formed by alternating face-sharing MO_6 (M=In^{3+}, Co^{3+}) trigonal prisms and CoO_6 octahedra. Each chain is surrounded by six chains, and neighboring chains are shifted with respect to each other by a 1/3*c (translation) along the c direction. The $B'O_6$ trigonal prism can be considered as the result of the substitution of two B and three interstitial oxygen atoms in the ABO_3 hexagonal perovskite by one B'. In such a structure, the height of the $B'O_6$ trigonal prism is

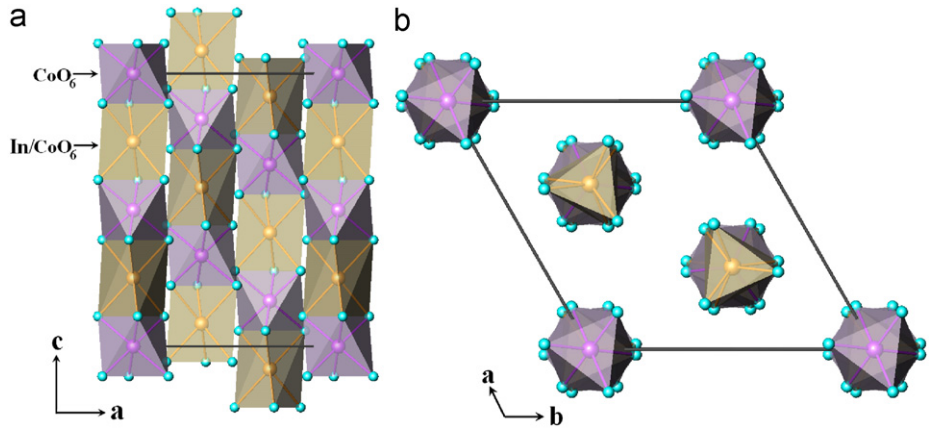

Fig. 4. Distribution of 1D chains in the structure of $Sr_3In_{0.9}Co_{1.1}O_6$ viewed along the directions [010] (a) and [001] (b).

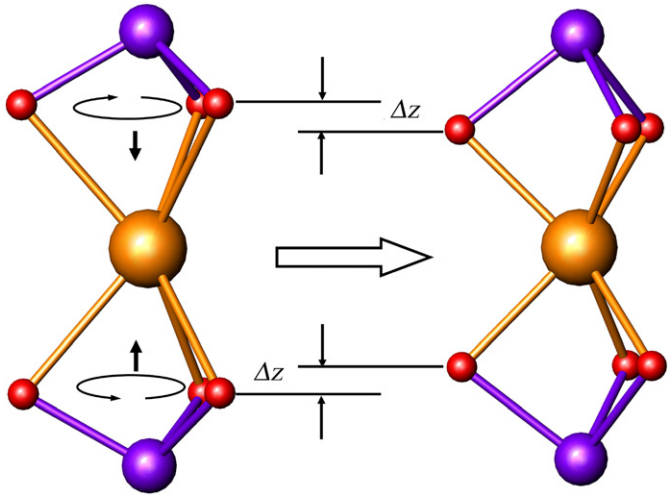

Fig. 5. Schematic pattern of the shift and rotation of oxygen atoms. The small red balls stand for oxide anions, the large and medium balls stand for B' (in trigonal prism) and B (in octahedron) cations, respectively. (For interpretation of the references to colour in this figure legend, the reader is referred to the web version of this article.)

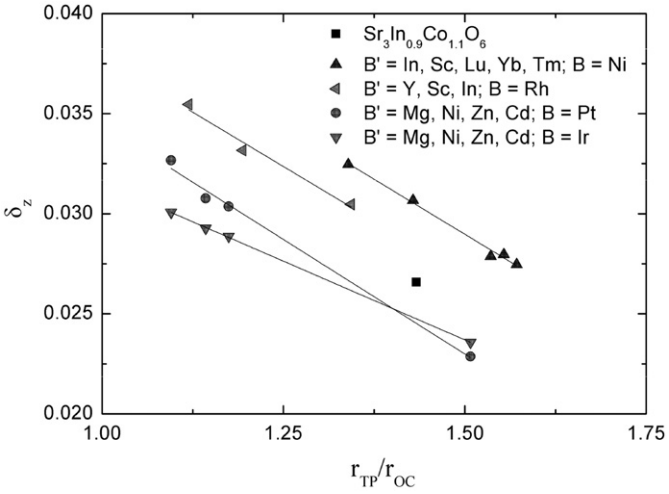

Fig. 6. Relative shift ($\delta_z = \Delta z/c$) in $Sr_3B'BO_6$.

roughly twice that of BO_6 octahedron. In real structures the oxygen atoms of $B'O_6$ rotate and shift with respect to B', and the shift distance and the rotation angle describe the deviation from the ideal coordination. Here the relative shift δ_z ($=\Delta z/c$), the quotient of the shift distance Δz (shown in Fig. 5) divided by c parameter, is used to compare the distortion of the chain. We summarized the structure data of some $Sr_3B'BO_6$ compounds [6,27–31] and found that δ_z had an approximately linear relationship with the ratio r_{TP}/r_{OC}; here r_{TP} and r_{OC} stand for the radius of B' and B cations, as shown in Fig. 6. The shift depends on the radii of B' and B atoms. The closer the B' and B atoms are, the more obvious the shift is. In $Sr_3B'BO_6$ [6,27–31], δ_z is in the range of 0.02–0.04. The distortion of the octahedron and trigonal prisms for $Sr_3In_{0.9}Co_{1.1}O_6$ is comparable to the others.

3.3. Magnetic properties of $Sr_3In_{0.9}Co_{1.1}O_6$

In $Sr_3In_{0.9}Co_{1.1}O_6$, only 1/10 of trigonal prismatic positions are occupied by Co^{3+}(HS); then the formula weight containing one mole of Co^{3+} (HS) is ten times of that of $Sr_3In_{0.9}Co_{1.1}O_6$ and the molar susceptibility of the Co^{3+} (HS) is calculated accordingly. The dependence of magnetic susceptibility on temperature is shown in Fig. 7. The plot of the inverse magnetic susceptibility to temperature fits Curie's Law very well, indicating that $Sr_3In_{0.9}Co_{1.1}O_6$ is paramagnetic. The neutron diffraction data of $Sr_3In_{0.9}Co_{1.1}O_6$ at low temperatures also confirm the paramagnetic behavior. The experiments carried out down to 1.5 K did not show any signs of

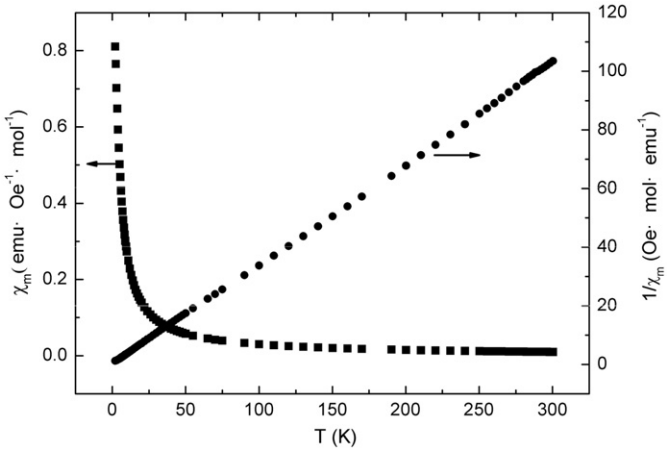

Fig. 7. Plots of magnetic susceptibility and its inverse with temperature for $Sr_3In_{0.9}Co_{1.1}O_6$.

long-range magnetic order. The Curie constant C is 2.9 $cm^3\ mol^{-1}\ K$. According to the equation $8C=g^2S(S+1)$, we can deduce that the g factor of Co^{3+} (HS) in $Sr_3In_{0.9}Co_{1.1}O_6$ is about 2.0.

The magnetism of Co^{3+}(HS) in $Sr_3In_{0.9}Co_{1.1}O_6$ is isolated instead of being coupled. Its nearest neighbor in the chain is Co^{3+}(LS) and the next nearest neighbor is In^{3+} with 90% possibility and Co^{3+}(HS) with 10% possibility. The increase of the content of Co^{3+}(HS) in trigonal prisms is helpful to the formation of segments of Co^{3+}(HS)–Co^{3+}(LS)–Co^{3+}(HS), and as a consequence enhances the interaction between Co^{3+}(HS) cations. Since in the system SrO–$InO_{1.5}$–CoO_x at 1000 °C, $Sr_3In_{0.9}Co_{1.1}O_6$ appears as a sharp compound, the content of Co^{3+} may be adjusted by the simultaneous substitution of Sr^{2+} by other cations.

4. Conclusions

In the investigation of the phase relations of the system SrO–$InO_{1.5}$–CoO at 1000 °C in atmosphere, a new ternary compound $Sr_3In_{0.9}Co_{1.1}O_6$, isostructural to $Ca_3Co_2O_6$, is revealed. The structure of $Sr_3In_{0.9}Co_{1.1}O_6$ is confirmed by Rietveld analysis of powder X-ray and neutron diffraction data. $Sr_3In_{0.9}Co_{1.1}O_6$ crystallizes in a trigonal system with the cell parameters $a=b=9.59438(3)$ Å, $c=11.02172(4)$ Å in the space group R-3c. Its structure contains a 1-D chain constructed by alternating face-sharing CoO_6 octahedra and $(In_{0.9}Co_{0.1})O_6$ trigonal prisms. The co-occupation of In^{3+} and Co^{3+} in the trigonal prism is evidenced by elementary analysis and determined by the refinement based on neutron diffraction data. In $Sr_3In_{0.9}Co_{1.1}O_6$, the Co^{3+}(HS) in trigonal prismatic positions are well separated by diamagnetic $Co^{3+}O_6$ octahedra and InO_6 trigonal prisms, such that the interaction between Co^{3+}(HS) is very weak, and no magnetic ordering was observed even down to 1.5 K. The magnetic measurements indicate that the compound is paramagnetic, and the susceptibility is consistent with 10% of the trigonal prismatic positions being occupied by Co^{3+} cations with the high spin $S=2$. Magnetic data give the value of the g factor of 2.0 for Co^{3+} (HS) in $Sr_3In_{0.9}Co_{1.1}O_6$.

Acknowledgments

This work is financially supported by the State Science and Technology Commission of China (Grant no. 2010CB833103) and National Natural Science Foundation of China (Grant no. NSFC 20821091). This work is partly based on experiments carried out at the Swiss Spallation Neutron Source SINQ, Paul Scherrer Institut, Villigen, Switzerland.

Appendix A. Supporting information

Supplementary data associated with this article can be found in the online version at doi:10.1016/j.jssc.2011.02.024.

References

[1] J.-G. Cheng, J.-S. Zhou, J.B. Goodenough, Phys. Rev. B 79 (2009) 184414-1–184414-6.
[2] J. Sugiyama, H. Nozaki, Y. Ikedo, K. Mukai, D. Andreica, A. Amato, J.H. Brewer, E.J. Ansaldo, G.D. Morris, T. Takami, H. Ikuta, J. Magn. Magn. Mater. 310 (2007) 2719–2721.
[3] Y.B. Kudasov, Phys. Rev. Lett. 96 (2006) 027212-1–027212-4.
[4] M.-H. Whangbo, D. Dai, H.-J. Koo, S. Jobic, Solid State Commun. 125 (2003) 413–417.
[5] W. Wong-Ng, G. Liu, J. Martin, E.L. Thomas, N. Lowhorn, J.A. Kaduk, J. Appl. Phys. 107 (2010) 033508-1–033508-6.
[6] K.E. Stitzer, J. Darriet, H.-C. z. Loye, Cur. Opin., Solid State Mater. Sci. 5 (2001) 535–544.
[7] T. Takami, H. Ikuta, U. Mizutani, Jpn. J. Appl. Phys. 43 (2004) 8208–8212.
[8] T. Takami, H. Nozaki, J. Sugiyama, H. Ikuta, J. Magn. Magn. Mater. 310 (2007) e438–e440.
[9] K. Takubo, T. Mizokawa, S. Hirata, J.-Y. Son, A. Fujimori, D. Topwal, D.D. Sarma, S. Rayaprol, E.-V. Sampathkumaran, Phys. Rev. B 71 (2005) 073406-1–073406-4.
[10] H. Fjellvåg, E. Gulbrandsen, S. Aasland, A. Olsen, B.C. Hauback, J. Solid State Chem. 124 (1996) 190–194.
[11] S. Aasland, H. Fjellvåg, B. Hauback, Solid State Commun. 101 (1997) 187–192.
[12] V. Hardy, M.R. Lees, O.A. Petrenko, D. McK. Paul, D. Flahaut, S. Hébert, A. Maignan, Phys. Rev. B 70 (2004) 064424-1–064424-7.
[13] R. Frésard, C. Laschinger, T. Kopp, V. Eyert, Phys. Rev. B 69 (2004) 140405(R)-1-4.
[14] E.V. Sampathkumaran, N. Fujiwara, S. Rayaprol, P.K. Madhu, Y. Owatoko, Phys. Rev. B 70 (2004) 014437-1–014437-4.
[15] R.V. Schenck, H. Mullerbu., Z. Anorg. Allg. Chem. 398 (1973) 24–30.
[16] K. Boulahya, M. Parras, J.M. González-Calbet, J. Solid State Chem. 145 (1999) 116–127.
[17] T. Takami, H. Ikuta, J. Appl. Phys. 103 (2008) 07B701-1-3.
[18] J.L. Sun, G.B. Li, Z.F. Li, L.P. You, J.H. Lin, Inorg. Chem. 45 (2006) 8394–8402.
[19] K. Iwasaki, T. Ito, T. Matsui, T. Nagasaki, S. Ohta, K. Koumoto, Mater. Res. Bull. 41 (2006) 732–739.
[20] Y. Takeda, R. Kanno, T. Takada, O. Yamamoto, M. Takano, Y. Bando, Z. Anorg. Allg. Chem. 540 (1986) 259–270.
[21] W.T.A. Harrison, S.L. Hegwood, A.J. Jacobson, J. Chem. Soc. Chem. Commun. (1995) 1953–1954.
[22] O. Gourdon, V. Petricek, M. Dusek, P. Bezdicka, S. Durovic, D. Gyepesova, M. Evain, Acta Crystallogr. B55 (1999) 841–848.
[23] S.E. Dann, M.T. Weller, J. Solid State Chem. 115 (1995) 499–507.
[24] C. Dong, J. Appl. Crystallogr. 2 (1999) 65.
[25] J. Rodríguez-Carvajal, Physica B 192 (1993) 55–69.
[26] W.F. Kuhs, in: A. Authier (Ed.), International Tables for Crystallography, vol. D, Kluwer Academic Publishers, Dordrecht, 2003, pp. 228–242.
[27] P. Núñez, S. Trail, H.-C. z. Loye, J. Solid State Chem. 130 (1997) 35–41.
[28] T.N. Nguyen, H.-C. z. Loye, J. Solid State Chem. 117 (1995) 300–308.
[29] C. Lampe-Önnerud, M. Sigrist, H.-C. z. Loye, J. Solid State Chem. 127 (1996) 25–30.
[30] G.V. Vajenine, R. Hoffmann, H.-C. z. Loye, Chem. Phys. 204 (1996) 469–478.
[31] R.C. Layland, S.L. Kirkland, P. Nunez, H.-C. z. Loye, J. Solid State Chem. 139 (1998) 416–421.